Computational homogenization method for the bending analysis of submarine power cables

Pan Fang[a,*]; Xiao Li[b]; Xiaoli Jiang[a]; Hans Hopman[a]; Yong Bai[c]

[a]Department of Maritime and Transport Technology, Delft University of Technology, Netherlands

[b]Institute of High Performance Computing (IHPC), Agency for Science, Technology and Research (A*STAR), 1 Fusionopolis Way, #16-16 Connexis, 138632, Singapore

[c]College of Civil Engineering and Architecture, Zhejiang University, Hangzhou, Zhejiang, P.R. China

P.Fang-1@tudelft.nl

Abstract. The complex structure and material property of a cable, particularly the stick-slip issue among its components pose the challenge for the bending analysis of submarine power cables. The calculation time and convergence problem of a full model makes the simulation unpractical during the design phase. This paper takes advantage of the peculiar structural property of helical components inside a cable, proposing a computational homogenization approach for analyzing the cable behavior under bending from global and local perspectives. This method assumes a macro model that is based on the theory of periodic beamlike structure, and a short-size micro model that is solved through a detailed finite element study. Results demonstrate the efficiency and capability of the proposed model that considers the structure nonlinearity and contact condition of a multi-layer cable with helical wires.

INTRODUCTION

Submarine power cables have played a key role in transporting electricity produced by wind turbines, current converters and other electricity generators. They consist of multi layers made of different materials. The most complex layer in a cable is usually the helical layer that is composed of numerous helical wires winding around by an angle. Except in submarine power cables, helical wires have also been used in flexible structures such as flexible pipes and umbilicals [1-3]. They usually serve as a structural layer to protect the inner layers from mechanical failure and meanwhile provide certain flexibility so that the flexible structure is able to bend to an aimed curvature. The difficulties in studying the structural behaviour induced by helical wires are not the structure itself, but also the contact issue among them and their neighbouring layers, especially when the cable is under bending where contact pressure varies on different areas.

Although analytical models have been developed for flexible structures, the practical contact situation inside the cable is impossible to be obtained through this method during the deformation

process, and therefore, it is usually assumed that the contact pressure is based on a state before bending, such as the contact state in tension[4]. The slip path of the helical wires is usually assumed to be geodesic or loxodromic in the previous studies[1]. However, the stick or slip state needs to be determined based on the contact pressure on the helical wires, and the analytical method fails to confirm that.

It is usually unpractical to run a full-scale finite element model of a complicated cable considering current computation capability. The studies regarding submarine power cables under axisymmetric loadings gradually appear recently[3, 5] where the helical wires can be simplified into beam element, which significantly reduces the calculation time. This simplification is acceptable since the slip phenomenon is not obvious in axisymmetric loadings and the contact can be ignored. However, this becomes different when the structure is under bending where the contact is intensive and is proved to have a significant influence on the final results[6]. A method to deal with this is to develop a special element that is capable to deal with contact, and the element should be efficient enough to cause calculation magnitude as less as possible[7]. An alternative is to apply the periodic boundary conditions by taking advantage of the helical symmetry of helical wires thanks to the computational homogenization[8]. This method was early developed to tackle the problem for composite structures[9] and are gradually extended to other structures such as helical ropes[10] and flexible pipes[11].

The main objective is to develop a short-size finite element model based on the periodic homogenization method to study the bending behaviour of a real submarine power cable. Section 2 introduces the homogenization theory followed by Section 3 that presents the implementation of the periodic boundary conditions. Section 4 gives the case study of a SPC by using the homogenization model aforementioned. In Section 5, the results from this model are validated through the bending test regarding four SPC samples, and the mechanical behaviour of the wires are discussed in detail. The obtained conclusions will benefit the practitioner and scholars who are studying the mechanical behaviour of SPCs.

1. Homogenization method for periodic beam-like structures

The computational homogenization method developed for periodic beam-like structures has been introduced by Patrice[10, 12]. For the completeness of the paper, the theory is described here in short.

Thanks to the periodicity in the axial direction of the helical structure, a short-size section is able to represent the whole structure after suitably applying the periodic boundary conditions on the investigated domain. An example of a structure from macroscopic to microscopic is given in Fig. 1. The macroscopic structure is a 1D Navier-Euler-Bernoulli-Saint-Venant beam problem[13] that can be decomposed into a series of microscopic 3D structure. The length l of the representative microscopic 3D model is determined by:

$$l = k\frac{p}{n} \tag{1}$$

Where $k \in \mathbb{N}$, p is the pitch length of the helical wire and n is the number of wires in this wire layer. The homogenization approach used in Patrice[12] is based on the asymptotic expansion method where two small parameters are involved: 1) the ratio of the microscopic length to the macroscopic length, and 2) the inverse of the structure slenderness (ratio of cable diameter to cable length). These two parameters are denoted ε:

$$\varepsilon \simeq \frac{l}{L} \simeq \frac{d}{L} \tag{2}$$

The microscopic scale y in Fig. 1 is introduced as $y = x/\varepsilon$. For the macroscopic problem, the relations among the variables are:

$$\begin{cases} div_y \sigma = 0 \\ \sigma = a(y) : e \\ e_{\alpha\beta} = e_{y_{\alpha\beta}}(u^{per}), [\alpha, \beta] = [1,2] \\ e_{13} = e_{y_{13}}(u^{per}) - y_2 E^T / 2 \\ e_{23} = e_{y_{23}}(u^{per}) + y_1 E^T / 2 \\ e_{33} = e_{y_{33}}(u^{per}) + E^E - y_\alpha E^{C_\alpha} \\ \sigma \cdot = 0 \text{ on } \partial Y \\ u^{per} \text{ per and } \sigma \cdot n \text{ anti-per} \end{cases} \quad (3)$$

Where a is the elastic moduli tensor, div_y the divergence operator, e_y the strain operator, σ the stress. E^E, E^T and E^{C_α} are respectively extension, torsion and curvatures from the macroscopic strain state. 'per' means *l*-periodic in variable y_3, while anti-per means that $\sigma \cdot n$ are opposite on opposite sides ∂Y^+ and ∂Y^- in the cable axial direction. The microscopic problem with imposed boundary conditions from macroscopic problem can be solved by using finite element method.

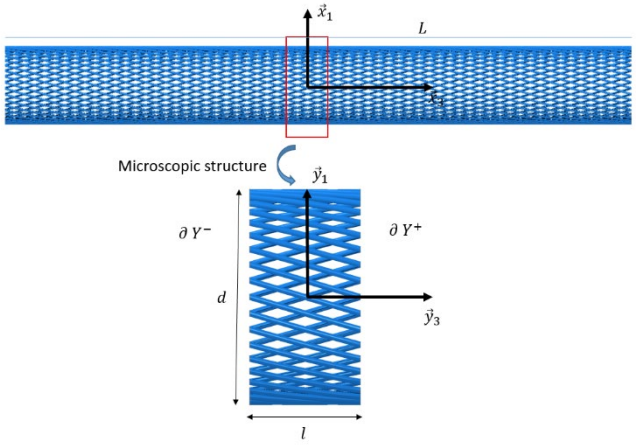

Fig. 1 Presentation of the relation between a macroscopic and microscopic structure regarding helical wires

2. Implementation of periodic boundary conditions

The microscopic problem is solved by finite element method. According to the approach proposed by [12], the discretized field u in the microscopic problem is determined from Eq. $(3)_{3\text{-}6}$, yielding:

$$\begin{cases} u_1 = u_1^{per} + \frac{1}{2} y_3^2 E^{F_1} - y_2 y_3 E^T \\ u_2 = u_2^{per} + \frac{1}{2} y_3^2 E^{F_2} + y_1 y_3 E^T \\ u_3 = u_3^{per} + y_3 E^T - y_\alpha y_3 E^{F_\alpha} \end{cases} \quad (4)$$

The periodic boundary conditions on u^{per} are dealt by connecting DOFs of opposite nodes on ∂Y^+ and ∂Y^-, as shown in Fig. 1. The six DOFs between the opposite nodes have the following relation:

$$\begin{aligned}
U_1^+ - U_1^- &= l(\overline{y}_3 E^{F_1} - y_2 E^T) \\
U_2^+ - U_2^- &= l(\overline{y}_3 E^{F_2} + y_1 E^T) \\
U_3^+ - U_3^- &= l(E^E - y_\alpha E^{F_\alpha}) \\
\theta_1^+ - \theta_1^- &= l E^{F_1} \\
\theta_2^+ - \theta_2^- &= l E^{F_2} \\
\theta_3^+ - \theta_3^- &= l E^T
\end{aligned} \tag{5}$$

Where U_i, θ_i are the translational and rotational DOFs, respectively.

The periodic boundary conditions can be inputted into finite element method by setting the DOFs on corresponding nodes. An efficient approach is by projecting the corresponding nodes on a virtual plane, as shown in Fig. 2. In the center of the virtual plane, there is a reference point R_p that is used to control the movement of all the projected nodes. In this way, the periodic boundary conditions are applied on the microscopic model.

The relation of the three RPs is implemented through the linear multi-point constraint equations in ABAQUS[14] which requires that a linear combination of nodal variables is equal to zero:

$$A_1 u_i^P + A_2 u_j^Q + \cdots + A_N u_k^R = 0 \tag{6}$$

Where u_i^P is a nodal variable at node P, degree of freedom of i; and the A_N are coefficients that define the relative motion of the nodes. In current FEM model, the equation among the three nodes in the left side is:

$$\mathbf{u}_{n_L} - \mathbf{u}_{n_M} - \mathbf{u}_{n_P} = 0 \tag{7}$$

The displacements of the dummy projected node $\mathbf{u}_{n_P}$ is obtained by rigidly constrained to the center node R_P by suing the rigid-body constraint equations:

$$\mathbf{u}_{n_P} = \mathbf{u}_{R_P} + \boldsymbol{\phi}_{R_P} \times \mathbf{X}_{n_P} \tag{8}$$

$$\boldsymbol{\phi}_{n_P} = \boldsymbol{\phi}_{R_P} \tag{9}$$

3. Case study

Sections 2 and Section 3 discusses the homogenization theory and the implementation of periodic conditions, respectively. This part presents the implementation of an SPC model under bending by setting the periodic boundary conditions. ABAQUS static general algorithm, where the dynamic effects are not considered, is selected for the analysis.

3.1. Cross section and material properties

The cross section of the studied SPC is shown in Fig. 3. The cable is simplified into six layers by ignoring the extremely thin layers such as copper shield and insulation shield. The cross section of the homogenization model is shown in Fig. 5.

The geometry and materials used in the simplified model is given in Table 1. Layer III is composed of 40 helical wires with the pitch length of 400mm. The material cooper has Young's modulus of 90 GPa, Poisson's ratio of 0.32 and yield strength of 130 MPa. However, XLPE and MDPE for the other layers are nonlinear material, and their properties are obtained through a series of material test. The strain-stress relation of these two materials after the manipulation by Ramberg-Osgood method[15] are presented in Fig. 4.

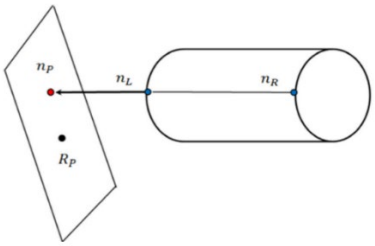

Fig. 2 Correspondence between a pair of nodes n_L and n_R on the two end-cross sections and the dummy projected node n_P, which is constrained to the reference node R_P [11]

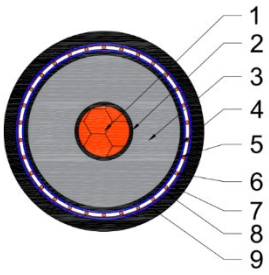

Fig. 3 Cross section of the SPC

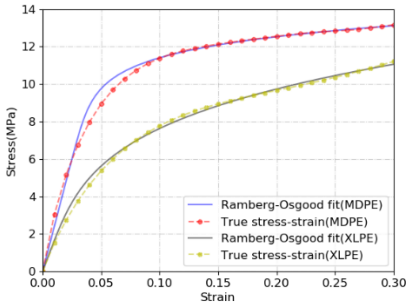

Fig. 4 Ramberg-Osgood fit of MDPE and XLPE

3.2. Mesh and interaction

C3D8R (An 8-node linear brick, reduced integration, hourglass control) is selected to mesh the cable components. For numerical consideration, the model doubles its length based on Eq.(1) and has a length of 20mm. In the axial direction, Layer I, Layer II and Layer IV have 14 elements, while the separated layers and the wires have 48 elements. This mesh strategy generates 1208688 elements and 2172939 nodes totally. The mesh is shown in Fig. 5.

Surface-to-surface algorithm is used to simulate the contact among all the components. The normal contact is set to hard contact and the friction coefficient is set to $\mu = 0.12$ [16] considering both the convergence and accuracy of the model.

3.3. Boundary conditions for a constant curvature

In order to form a constant curvature for the whole cable, the middle nodes in the center line of the middle copper conductor are defined as a series of sets and connected to the other nodes on the corresponding cross section, as shown in Fig. 6. The defined set are coupled to the cross section in the following way. These nodes are coupled to Layer I, Layer II and Layer VI in the U3 and UR1 directions, while they are coupled to Layer III and Layer V in the all directions, as shown in Fig. 7, to create an even curvature around the helical wires for the consideration of convergence.

The middle node is totally fixed since it is used to control the symmetric face of the cable. A rotation angle and a displacement are applied on the most left node to bend the cable. The loading situation at the most right node is the same except the rotation angle is applied in the opposite direction. The boundary conditions for the three control nodes are given in Table 2. By controlling the movements of the defined center nodes to obtain a constant curvature, a pure bending of the cable can be simulated.

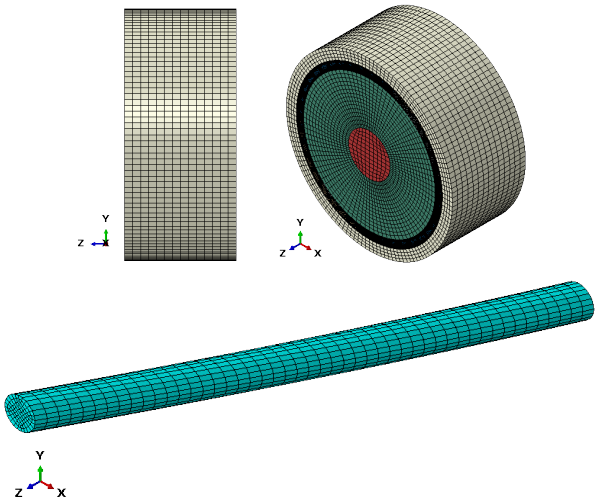

Fig. 5 Meshing of the SPC

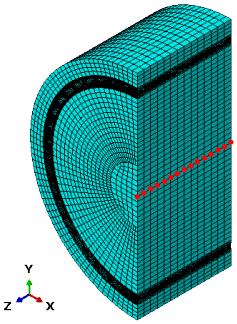

Fig. 6 The master nodes in the center line of the copper conductor

3.4. Periodic conditions on the helical wires

As shown in Fig. 8, reference points(RPs) are built in the center of each wire cross section on both sides and the middle. The movements of the nodes in the wire cross section is controlled through this RP that coupled to all the cross-section nodes. The RPs on the left, right and the dummy RPs on the projected plane constitute a relation given in Eq. (8). The dummy projected RP is in the same location as the RP on both sides, therefore, they are overlapped in Fig. 8.

n_L, n_M and left n_P constitute a relation in Eq. (8). meanwhile, n_R, n_M and right n_P constitute a relation in Eq. (8) as well to build up a symmetrical surface. These nodes are on the same axis. n_L and n_R are the dependent nodes while n_M and n_P on both sides are master nodes, as shown in Fig. 9. There are 40 helical wires here in this case, which makes 40×6 constraints on the left side and 40×6 constraints on the right side, therefore, totally 480 equation constraints in the model.

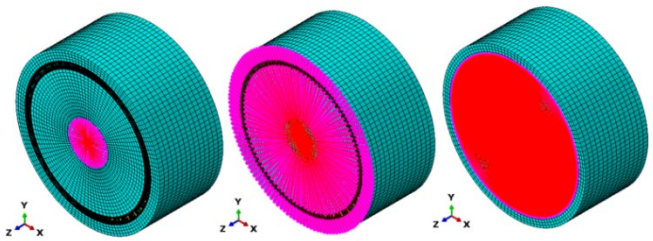

Fig. 7 The coupling set regarding the cylinder layers

Table 2 The boundary condition for the three control nodes

	Left control node	Middle control node	Right control node
U1	1	1	1
U2	u_y	1	u_y
U3	0	1	0
U4	θ_x	1	$-\theta_x$
U5	1	1	1
U6	0	1	0

Note: 1 means the corresponding DOF is constraint and 0 means it is free

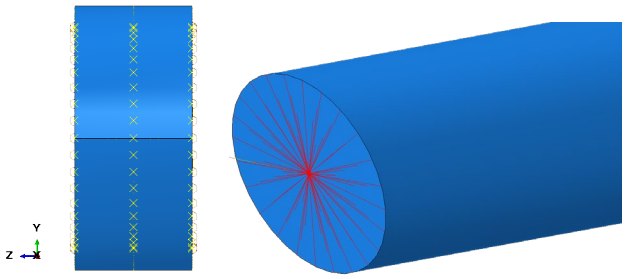

Fig. 8 Two groups of RPs on the left side and right side(a) & The coupling setting of RP to the corresponding cross section

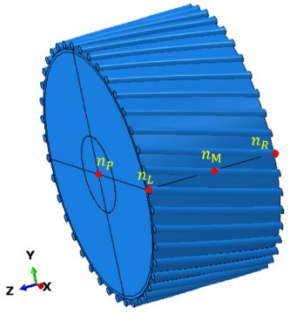

Fig. 9 The periodic boundary conditions on the homogenization model for a group of constraint nodes

4. Results and discussions

The overall cable behavior, i.e., the curvature-moment relation from the FEM method is extracted and compared with the test results from four cable samples, as shown in Fig. 10. The overall trend of the curve from the FEM method is the same as the test curves, and it is observed that the slope of the curves, i.e., the bending stiffness, from the test agrees better with the FEM result in the beginning phase. However, as the curvature increases, the bending moment in the test becomes smaller than the FEM moment. This is likely to be caused by the slip situation inside the copper conductor, as the conductor itself is composed by many helical ropes and there are certain gaps that might induce the slip. This slip situation can not be reflected in the FEM method as the geometry details of the copper conductor are not built. When the curvature reaches 0.01mm^{-1}, most of the copper conductor yields and the stress of the conductor is much higher than the other components, as illustrated in Fig. 10, which illustrates the copper conductor contributes more to the bending.

The bending moment, as discussed above, is mainly contributed from the copper conductor. The helical wires do not play a dominant role in affecting the overall bending behavior, however, the stress state and behavior of itself are of interest to engineers. The outermost sheath and conductor are removed to show the movement and stress of all the wires clearly in Fig. 11. It is observed that the stress distribution over the helical wires is very even, proving that the edge effect from the periodic boundary condition model can be neglected. The Mises stress on a wire are not the same everywhere but has a pattern. Fig. 12 illustrates the axial stress of all the wires, which shows the axial stress around the wire itself is changing, where the upper part is tensioned while the below part is compressed.

To investigate the displacement of all the wires around the cable circle, three paths composed of the nodes in the middle of wire cross sections are built, as shown in Fig. 13. The displacements of the nodes along the path are extracted and shown in Fig. 14. It is found the displacements of the wires in the extrados and intrados are smallest and near to zero, while the displacements of the wires in the center plane are the largest. This corresponds to the analytical model that indicates the wire in the extrados and intrados still adhere to their original location after bending.

Table 1 Parameters and materials used in the simplified model.

Layers	Thickness(mm)	Outer diameter(mm)	Materials
I	-	11.4	Copper
II	12.75	36	XLPE
III	0.45	36.9	MDPE
IV	1.15	39.2	Copper
V	0.45	40.1	MDPE
VI	2.7	45.5	MDPE

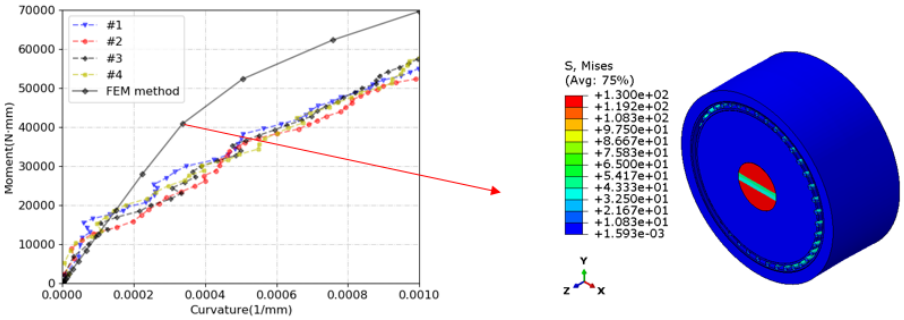

Fig. 10 Curvature-moment from FEM method and test results

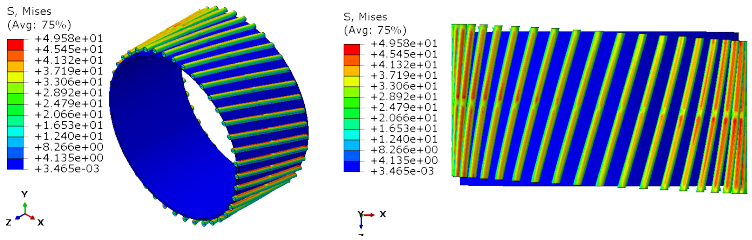

Fig. 11 The detail of the helical wires on the neighboring layer

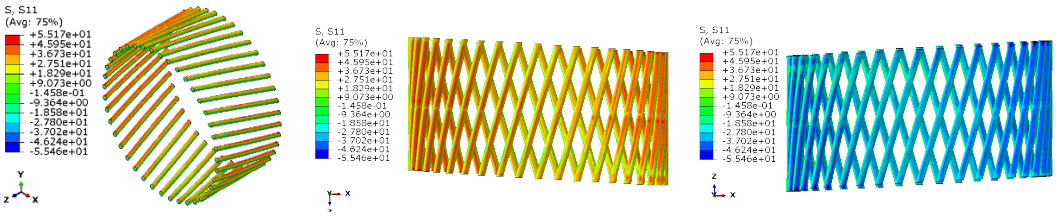

Fig. 12 Axial stress of the wires

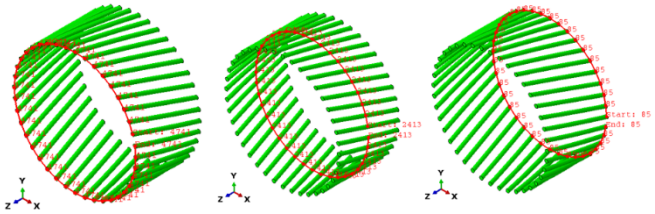

Fig. 13 Node path around the cross section (Left, Middle & Right)

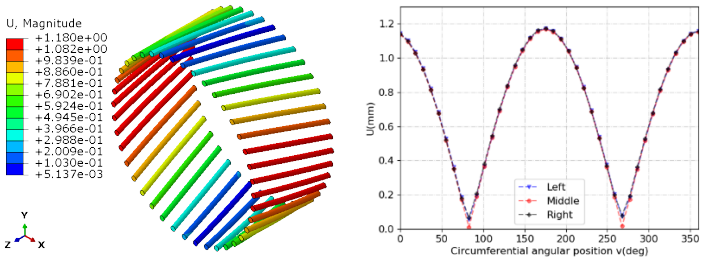

Fig. 14 The displacement contour of helical wires and the displacement of the wire nodes along the circumferential angular position

CONCLUSIONS

In this study, a short-size FE model of a power cable is built based on computational homogenization method to study the mechanical behavior from global and local perspectives. The overall curvature-moment relation from the FE model is validated through the test results, and the reason for the discrepancy between the two methods is discussed. The detailed mechanical behavior of the helical wires are presented and discussed, including the displacement and the stress after the cable reaches an aimed curvature. The findings are concluded below:

1) The bending moment from the homogenization model agrees better with the test results at the beginning of the bending, however, the moment from the model becomes higher when the curvature gradually increases. This might be caused by the slip issue inside the copper conductor.

2) The axial stress around the cross section of each wire is not the same, however, the upper part mainly bears tension while the below part mainly bears compression. The difference phenomenon is more obvious around the neutral plane of the cable.

3) The displacements of the helical wires around extrados and intrados are near to zero. The displacements of their counterparts around the cable neutral plane are the largest after bending.

The proposed FEM model based on homogenization method is validated by test results. This model can be used to study the global and local behavior of SPC under tension, bending or combined loadings. A more mature model including other functions can also be developed based on current model, which can provide a meaningful simulation tool for relevant practitioners and engineers who are working on SPCs.

References

1. Sævik, S., *On stresses and fatigue in flexible pipes.* 1992.
2. Witz, J. and Z. Tan, *Rotary bending of marine cables and umbilicals.* Engineering structures, 1995. **17**(4): p. 267-275.
3. Fang, P., et al., *Mechanical responses of submarine power cables subject to axisymmetric loadings.* Ocean Engineering, 2021. **239**: p. 109847.
4. Papailiou, K.O., *Bending of helically twisted cables under variable bending stiffness due to internal friction, tensile force and cable curvature.* Doctor of Technical Sciences thesis, ETH, Athens, Greece, 1995.
5. Chang, H.-C. and B.-F. Chen, *Mechanical behavior of submarine cable under coupled tension, torsion and compressive loads.* Ocean Engineering, 2019. **189**: p. 106272.
6. Vaz, M., et al. *Experimental determination of axial, torsional and bending stiffness of umbilical cables.* in *Proceedings of the 17th International Offshore & Arctic Engineering Conference (OMAE'98)*. 1998.
7. Sævik, S., *Theoretical and experimental studies of stresses in flexible pipes.* Computers & Structures, 2011. **89**(23-24): p. 2273-2291.
8. Yuan, Z. and J. Fish, *Toward realization of computational homogenization in practice.* International Journal for Numerical Methods in Engineering, 2008. **73**(3): p. 361-380.
9. Geers, M.G., V.G. Kouznetsova, and W. Brekelmans, *Multi-scale computational homogenization: Trends and challenges.* Journal of computational and applied mathematics, 2010. **234**(7): p. 2175-2182.
10. Cartraud, P. and T. Messager, *Computational homogenization of periodic beam-like structures.* International Journal of Solids and Structures, 2006. **43**(3-4): p. 686-696.
11. Rahmati, M., H. Bahai, and G. Alfano, *An accurate and computationally efficient small-scale nonlinear FEA of flexible risers.* Ocean Engineering, 2016. **121**: p. 382-391.
12. Ménard, F. and P. Cartraud, *Solid and 3D beam finite element models for the nonlinear elastic analysis of helical strands within a computational homogenization framework.* Computers & Structures, 2021. **257**: p. 106675.
13. Xing, Y., et al., *A Novel Efficient Prediction Method for Microscopic Stresses of Periodic Beam-like Structures.* Aerospace, 2022. **9**(10): p. 553.
14. Abaqus, V., *6.14 Documentation.* Dassault Systemes Simulia Corporation, 2014. **651**: p. 6.2.
15. Ramberg, W. and W.R. Osgood, *Description of stress-strain curves by three parameters.* 1943.
16. Lukassen, T.V., et al., *Tension-bending analysis of flexible pipe by a repeated unit cell finite element model.* Marine Structures, 2019. **64**: p. 401-420.